CHAPTER VI
OBSERVATION OF RHEOLOGICAL PROPERTIES AND EXTRUDATE SWELL OF ISOTACTIC POLYPROPYLENE- TITANIUM DIOXIDE NANOCOMPOSITES

ABSTRACT

The TiO_2 nanoparticles filled in iPP matrix are observed the rheological properties and the extrudate swell phenomena in various amounts of filler loading from 5 to 30 wt% during capillary extrusion process. Neat iPP as well as the composites exhibited shear thinning pseudoplastic behavior. The TiO_2 nanaparticles treated the surface by stearic acid and exhibited the hydrophobic property, significantly reduced the rate of wall shear stress changing when increased amount of fillers as compared on hydrophilic surface composites. In various type of fillers, the shear viscosity on apparent shear rate presented not difference as much. The extrudate swell were reduced with increasing amount of fillers due to its will be blocked the elastic recovery of the composites. The hydro phobic surface TiO_2 nanocomposites presented the critical of the extrudate swell. These suggested that the critical point is maximized for good dispersion and distribution. The relationship of extrudate swell was increased linear function on the wall shear stress. In various types of the nanocomposites, the elongational viscosity and tensile stress as a function on elongational rate were investigated. Both neat iPP and the composites were presented the elongational viscosity on the elongational rate not difference as much. But, various amounts of fillers, the slope of tensile stress on elongational rate of nanocomposites were increased with increasing amount of fillers and maximum on 30 wt%. Finally, hydrophobic, the type of surface modification on nanoparticles, has more effective on elongational flow than shear flow.

Key-words: polymer nanocomposites; capillary rheometer; polymer rheology; extrudate swell; TiO_2 nanoparticles; shear viscosity; elonagtional viscosity.

6.1 INTRODUCTION

At the present time, special attention is devoted to the reinforcement of thermoplastic materials by using their mixer containing organic fillers on nano-sizes. Such an approach renders it possible to modify commercial thermoplastics properties so as to create essentially new engineering materials [1-5].

The properties of the composites are determined by properties of the matrix, shape or size of the filler particles, volume fraction of the constituent phases, and the degree of dispersion [6,7]. The interactions between the polymer molecules and the filler surface molecular conformation and molecular mobility are responsible for the occurrence of an interphase. The structures of the inter-phase are extremely important. Its can be modified by interfacial additives such as coupling agents and grafted polymer. In the manufacture of paints, plastics, elastomers, adhesives, good dispersion of pigments and fillers is essential for producing a high quality product. Titanium dioxide (TiO_2) is one of the most important organic fillers not only used for many polymers especially in coating, rubber, and plastic application but their also worked as white color master batch [8], thermal instability, frame retardant, and anti oxidant [9].

The rheology of composites was very interesting and strongly controlled the properties of final product [7,10,11,12]. The processing of flow conditions and microstructure developments are widely topics on the research. Lei et al. [8] investigated time dependent rheological behavior of LDPE filled white color masterbatchs (TiO_2) under dynamic stress field. It was found the experimental both high frequency and temperatures, more pronounced the viscosity increased. And the 30 wt% of TiO_2 content was critical to obvious time dependent behavior. The viscosity increased with increasing the time. It should be relate to the formation of hard shell around the melt sample during the test. White J. L. [13] studied the elongational flow of concentrated suspensions of TiO_2 in PS melts. The results suggested that highly filled compound exhibit enhanced elongational viscosity and instability in elongational flow. The author [10] proved the rheological properties of $CaCO_3$ nanoparticles filled iPP in various amount of fillers. The result shows an increased of wall shear stress and shear viscosity, which increase amount of fillers,

but. the extrudate swell was decreased. The surface coating has more affective on extrudate swell. The linear relationships of extrudate swell on wall shear stress are occurred. And, the slope value of linear function depends on the type of surface modification.

It is our purpose in the present paper to make carefully investigations the rheological properties as the shear, elongational, and extrudate swell of the nanocomposites various types of surface modification.

6.2 EXPERIMENTAL DETAILS

Materials

The general purpose PP homopolymer resin used as matrix polymer component include Polypropylene (PP) HP 400K was supplied by HMC Polymers Co., Ltd (Rayong Thailand) [14]. Specific properties of the resin, provide by ASTM and DIN standard for laboratory, are as follows, MFR (2.16kg at 190°C)= 4, density= 0.9 gcm^{-3}, tensile strength at yield= 33 nmm^{-2}, elongation at yield = 10%, flexural modulus = 1400 MPa, and notched izod impact strength at 23 °C = 30. Three types of TiO_2 nanoparticles were supplied by Advanced Nanotechnology Co., Ltd. (Samutprakarn Thailand) [15]. The specific properties are summarized on table 6.1.

Compounding

TiO_2 nanoparticles were dried in an oven at 80°C for 24 h and then pre-mixed with iPPpellets in a tumble mixer for 20 min in various compositional ratios (i.e. 5, 10, 20, and 30 wt%). The compounding were then fed in to COLLIN ZK25 self wiping, co-rotating twin screw extruder operated at a screw speed of 80 rpm and temperature profile of 190°C (die zone), 190°C (zone 5), 185°C (zone 4), 180°C (zone 3), 175°C (zone 2), and 100°C (feed zone). The extrudate was rapid cooled in water bath and cut into pellet form by a Planetrol 075 de pelletizer.

Rheological measurements

Capillary rheometer (CEAST Rheologic 5000 twin bore capillary rheometer) was used to measure shear and elongational behavior of samples. The dimensions of instrument were 15 and 300 mm on diameter and length of the barrel, the L/D ratios of die series selected on 10/2 and 30/2, respectively, testing temperature was set on 190 $^{o}C \pm 0.5^{o}C$, hold on time and hold on pressure for stages 1, 2, and 3 produced 230 sec and 10, 20 and 30 Pa, respectively. Data corrections were based on Bagley's, Rabinowitsch's correction [16,17] and Cogswell's convergence flow [17-20]. The average overall extrudate swelling was measured on KEYENCE VG laser analytical device.

6.3 RESULTS AND DISCUSSION

Dependence of wall shear stress on apparent shear rate for neat iPP and iPP filled with various amount of TiO_2 nanoparticles, CYU 201, CYU 202, and CYO 203 are illustrated in fig. 6.1. In the whole rang were analyzed (i.e. ca. 50-600 s^{-1}), both neat iPP and iPP compounds exhibited shear thinning behavior which non linear increased of wall shear stress as increasing shear rate. The results of fig. 6.1 a, b, and c show that the wall shear stress of iPP composites was greater than neat iPP and its maximum on 30 wt %.

According to fig. 6.1a and 6.1b, interestingly, amount of 30 wt% of fillers, are found the plateau of the flow curve appeared on 300-400 s^{-1} of shear rate. They could be inferred to critical shear stress point. While, the CYU 203 nanocomposites disappeared (see fig. 6.1c). The different of both results are greatly depended on the type of nanoparticle surface modification. CYU 203 nanoparticles were treated to form hydrophobic surface but other nanoparticles exhibited hydrophilic. Not only these results showed differently but the rate of change of wall shear stress values also confirm their. Generally, in the same rate, CYU 203 composites have less value than CYU202 and CYU 201 due to the better dispersion and distribution than the other compound. Comparatively, Fig. 6.2a and 6.2b shows the results of wall shear stress on apparent shear rate amount of 5 wt% and 30 wt%, respectively. Clearly, CYU 203

composites various compositions from 5 to 30 wt% was lower amount of stress than CYU 201 and CYU 202. The stress different was increased with influenced amount of fillers and maximum differences on 30 wt%.

Fig. 6.3a, b, and c shows the shear viscosity as a function of the real shear rate of CYU201, CYU202, and CYU 203 composites, respectively. All of type of composites presented the decreasing non linear manner as a function of the real shear rate follow to the behavior of pseudo plastic materials. The viscosity of all composites showed not different as much in the same rate but it can be seen little bit higher shear viscosity of 30 wt% than others.

Fig. 6.4 illustrates dependence of percentage of extrudate swell on apparent shear rate for neat iPP and iPP filled Tio_2 nanoparticles, CYU 201, CYU 202, CYU 203 (see fig. 6.4a, b, and c) respectively. Generally, the percentages of extrudate swell were increased non linear manner with increasing the apparent shear rate. Then the addition of TiO_2 nanoparticles reduced the extrudate swell. An increasing the weigh of filler contents affect to decrease the swelling. The author [10] reported a similar observation on iPP/$CaCO_3$ nanocomposites and suggested the results that the limit mobility of the matrix molecular chains due to the presence of the nanoparticles, the elastic recovery during leaved the die could be blocked. Interestingly, CYU 203 on 30wt% (see fig. 6.4c) was not following. The percentage of extrudate swell was decreased with increasing amount of fillers ranging from neat iPP, 5 wt%, 10 wt%, and minimum on 20 wt%. But in case of 30 wt%, it was influenced more over neat iPP. It could be infer to high filler contents, CYU 203, the hydrophobic surface nanoparticles could interact to form agglomerates when their added more over the limit of the dispersion of the filler contents. So that, the presence of TiO_2 nanoparticles within iPP matrix may not be as effective in the limiting the movement of the molecules during extrusion. The results can be confirmed on fig. 6.5, it was showed the percentage of the extrudate swell as a function of apparent shear rate on 10 mm of die length (L/D =5). It presented similarly behavior of 30 mm of die length.

Fig. 6.6 shows dependence of extrudate swell as a function of the wall shear stress for CYU 201, CYU 202, and CYU 203 composites of various filler contents from 5 to 30 wt%. Generally, for overall results, the extrudate swell exhibited a

linear relationship with the wall shear stress. It have been found by many authors [10,21,22]. The slope values of the results (see fig. 6.6a, b, and c) were not changed as much. But, the differences of all results between 5 to 30 wt% have significant. CYU 203 (see fig. 6.6c) was lower ranging value than those other composite. The extrudate values from 5 to 30 wt% were more closely than 201 and 202 composites. These imply nanofillers treated by hydrophobic surface less affect to the rheological behavior of the polymer matrix.

Comparatively, the L/D ratios of 15, the percentage of extrudate swell as a function of shear stress in various types of fillers was shows on fig. 6.7a and b, respectively. According fig. 6.7a, 5 wt% of fillers, not only TiO_2 nanoparticles with hydrophobic surface treatment (CYU 203) exhibited slightly greater than those types. But they also increased with influencing amount of filler and maximum differences on 30 wt% of fillers (see fig. 6.7b). The L/D ratios of 5 have been observed on fig. 6.8a and 6.8b. It presented similarly behavior from L/D ratio of 15. It should be suggested that the hydrophobic surface treatment of nanoparticles TiO_2 have effective in die series for this experiments.

Fig. 6.9 illustrated dependence of elongational viscosity on the elongational rate of CYU 203 composites in various amounts of fillers. An increasing the elongational rate, the elongational viscosity was non linear decreased. Comparatively, amount of fillers, neat iPP and composites presented the viscosity value not difference as much. The other composites exhibited similarly behavior. Fig. 6.10 shows the relationship between the tensile stress on elongational rate of neat iPP and CYU 203 composites in various amounts of fillers. It was found the tensile stress increased non linear manner with increasing the elongational rate. The slope values of the composites were greater than neat iPP following amount of fillers and maximum on 30 wt%. The result could be suggested that the nanocomposites with presence on the PP matrix their will be blocked the chains to slip apart when the stretching force occurred.

Comparatively, various types of fillers, fig. 6.11 showed the relationship of elongational viscosity on elongational rate at 5 wt% and 30wt%. As low as concentration of fillers (see fig. 6.11a), CYU 203 composites exhibited slightly greater than CYU 201 and CYU 202, respectively. At high concentration of fillers

(see fig. 6.11b), the elongational viscosity was significantly difference as the same elongational rate. Except on the high rate, the viscosity of all compositions may collapse each others. these results could be described not only the effects of surface modification on nanoparticles, their have more effective on elongational viscosity than shear viscosity but also indicated the nanoparticles on the polymer matrix have more effect on the rheological properties in which depended on operation mode.

The results on fig. 6.12 showed the comparison on the type of fillers on 5 and 30 wt% (fig. 6.12a and b).Tensile stress as a function of elongational rate. The CYU 203 composites exhibited greater stress value than CYU 201 and 202 at the same rate. The results showed the opposite of the shear mode in wall shear stress on the shear rate and imply the surface treatments of the nanomaterials have more effective on the elongational mode.

6.4 CONCLUSION

In the whole rang were analyzed, neat iPP and composites exhibited shear thinning pseudoplastic behavior. The TiO_2 nanaparticles treated the surface by stearic acid and exhibited the hydrophobic property, significantly reduced the rate of wall shear stress changing when increased amount of fillers as compared on hydrophilic surface composites. The shear viscosity on apparent shear rate of all samples presented not difference as much. Apparently, the extrudate swell was reduced with increasing amount of fillers due to its will be blocked the elastic recovery of the composites. The hydrophobic surface TiO_2 nanocomposites presented the critical of the extrudate swell and may suggest that the critical point is maximized for good dispersion and distribution of nanofillers in the polymer matrix. The relationship of extrudate swell was increased linear function on the wall shear stress. In various types of nanocomposites, the elongational viscosity and tensile stress as a function on elongational rate were investigated. Both neat iPP and the composites were presented the elongational viscosity on the elongational rate not difference as much. But, various amounts of fillers, the slope of tensile stress on elongational rate of nanocomposites were increased with increasing amount of fillers and maximum on

30 wt%. Finally, hydrophobic, the type of surface modification on nanoparticles, has more effective on elongational flow than shear flow.

6.5 ACKNOWLEDGMENTS

The authors would like to acknowledge the Asahi Glass Foundation on Overseas Research Grant for financial supported.

Partial supports received from the Petroleum and Petrochemical Technology Consortium (through a governmental loan from the Asian Development Bank) and from the Petroleum and Petrochemical College, Chulalongkorn University are gratefully acknowledged.

6.6 REFERENCES

[1] G. Schmidt, M. Malwitz, Current Opinion in Colloid and Interface Science 8 (2003) 103.

[2] L. Incarnato, P. Scarfato, L. Scatteia, D. Acierno, Polymer 45 (2004) 3487.

[3] C.M. Chan, J. Wu, J.X. Li, Y.K. Cheung, Polymer 43 (2002) 2981.

[4] S.Y. Gu, J. Ren, Q.F. Wang, Journal of Applied Polymer Science 91 (2004) 2427.

[5] T.D. Fornes, P.J. Yoon, H. Keskkula, D.R. Paul, Polymer 42 (2001) 9929.

[6] M. Arellano, I. M. Zloczower, D. L. Feke, Powder Technology 84 (1995) 117.

[7] P. V. Puyvelde, S. Velankar, P. Moldenaers, Current Opinion in Colloid and Interface Science 6 (2001) 457.

[8] C. Lei, D. Chen, R. Huang, G. Li, Y. Lu, Journal of Applied Polymer Science 85 (2002) 2793.

[9] G. I. Titelman, Y. Gonen, Y. Keidar, S. Bron, Polymer Degradation and Stability 77 (2002) 345.

[10] R. Dangtungee, J. Yun, P. Supaphol, Polymer Testing 24(2005) 2.

[11] N. Sombatsompop, R. Dangtungee, Journal of Materials Science Letters 20 (2001) 1405.

[12] N. Sombatsompop, R. Dangtungee, Journal of Applied Polymer Science 82 (2001) 2525.

[13] J. L. White, H. Tanaka, Journal of Applied Polymer Science 26 (1981) 579.

[14] Available from http://www.hmcpolymer.com/products/Homo_/HP-400_files.

[15] Available from http://www.advnano.com/products

[16] J.A. Bryson, Flow Properties of Polymer Melts, Van Nostrand Reinhold, New York, 1970

[17] F. N. Cogswell, Polymer Melt Rheology, wood head publishing, London, 1994.

[18] Ceast. S.P.A., Instruction Manual Handout of Visual Rheo, Pianezza,Italy.

[19] J. C. Huang, Z. Tao, Journal of Applied Polymer Science 87 (2003) 1587.

[20] M. E. Mackay, G. Astarita, Journal of Non Newtonian Fluid Mechanics 70 (1997) 219.

[21] J.Z. Liang, Polymer Testing 21 (2002) 927.

[22] J.Z. Liang, Polymer Testing 23 (2004) 441.

6.7 LIST OF FIGURE

Figure 6.1 Wall shear stress as a function of apparent shear rate for neat iPP and iPP filled with (a) CYU 201 and (b) CYU 202 (c) CYU 203 of TiO_2 nanoparticles in various amount of fillers.

Figure 6.2 Wall shear stress as a function of apparent shear rate for iPP filled with (a) 5 and (b) 30 wt.% of CYU 201, CYU 202, and CYU 203 TiO_2 nanoparticles.

Figure 6.3 Shear viscosity as a function of real shear rate for neat iPP and iPP filled with (a) CYU 201 and (b) CYU 202 (c) CYU 203 of TiO_2 nanoparticles in various amount of fillers.

Figure 6.4 Percentage of extrudate swell as a function of apparent shear rate for neat iPP and iPP filled with (a) CYU 201 and (b) CYU 202 (c) CYU 203 of TiO_2 nanoparticles in various amount of fillers.

Figure 6.5 Percentage of extrudate swell as a function of apparent shear rate for neat iPP and iPP filled with CYU 203 of TiO_2 nanoparticles in various amount of fillers on 10 mm of die length (L/D = 5).

Figure 6.6 Percentage of extrudate swell as a function of wall shear stress for neat iPP and iPP filled with (a) CYU 201 and (b) CYU 202 (c) CYU 203 of TiO_2 nanoparticles in various amount of fillers.

Figure 6.7 Percentage of extrudate swell as a function of wall shear stress for iPP filled with (a) 5 and (b) 30 wt% of CYU 201, CYU 202, and CYU 203 TiO_2 nanoparticles on 30 mm of die length (L/D = 15).

Figure 6.8 Percentage of extrudate swell as a function of wall shear stress for iPP filled with (a) 5 and (b) 30 wt% of CYU 201, CYU 202, and CYU 203 TiO_2 nanoparticles on 10 mm of die length (L/D = 5).

Figure 6.9 Elongational viscosity as a function of elongational rate for neat iPP and iPP filled with CYU 201 of TiO_2 nanoparticles in various amount of fillers.

Figure 6.10 Tensile stress as a function of elongational rate for neat iPP and iPP filled with CYU 203 of TiO_2 nanoparticles in various amount of fillers.

Figure 6.11 Elongational viscosity as a function of elongational rate for filled with (a) 5 and (b) 30 wt% of CYU 201, CYU 202, and CYU 203 TiO_2 nanoparticles on 30 mm of die length (L/D = 15)

Figure 6.12 Tensile stress as a function of elongational rate for filled with (a) 5 and (b) 30 wt% of CYU 201, CYU 202, and CYU 203 TiO_2 nanoparticles on 30 mm of die length (L/D = 15).

Table 6.1. Specific properties of the TiO_2 nanoparticles

Item	CYU 201	CYU 202	CYU 203
Average particle size (nm)	50	50	50
Crystal type	Rutile	Rutile	Rutile
Content of TiO_2 (%)	98	95	92
Specific surface area (m^2/g)	>35	>35	>35
Surface properties	Hydrophilic	Hydrophilic	Hydrophobic
Surface treatment agent	/	SiO_2	Fatty acid

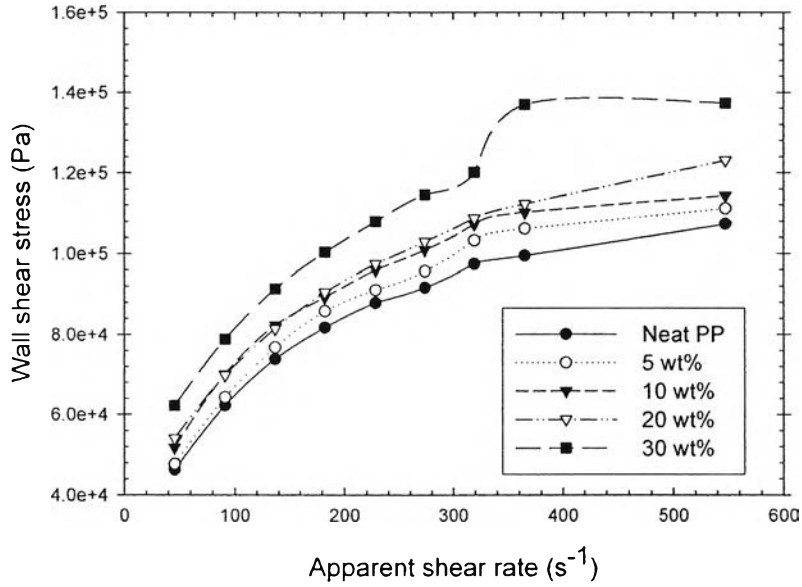
1.6e+5
1.4e+5
1.2e+5
1.0e+5
8.0e+4
6.0e+4
4.0e+4
Wall shear stress (Pa)
0
100
200
300
400
500
600
Apparent shear rate (s-1)
Neat PP
5 wt%
10 wt%
20 wt%
30 wt%

(a)

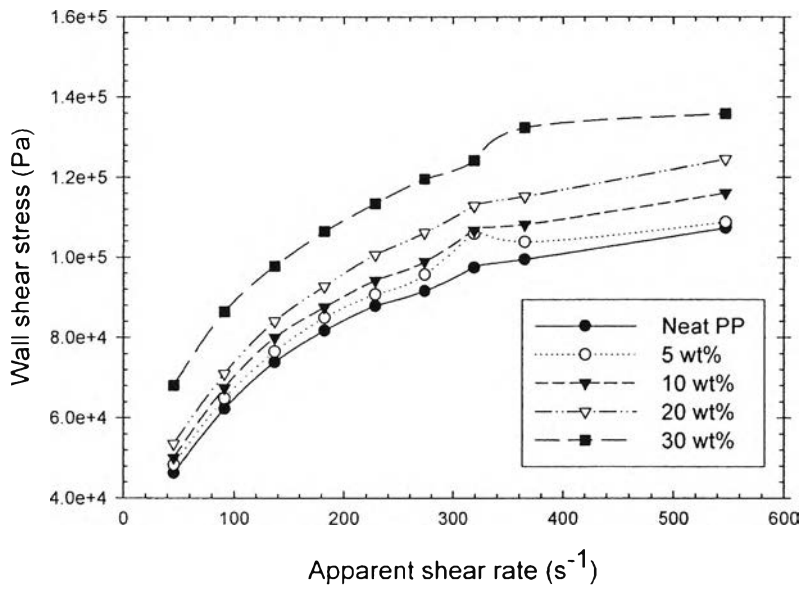
1.6e+5
1.4e+5
1.2e+5
1.0e+5
8.0e+4
6.0e+4
4.0e+4
Wall shear stress (Pa)
0
100
200
300
400
500
600
Apparent shear rate (s-1)
Neat PP
5 wt%
10 wt%
20 wt%
30 wt%

(b)

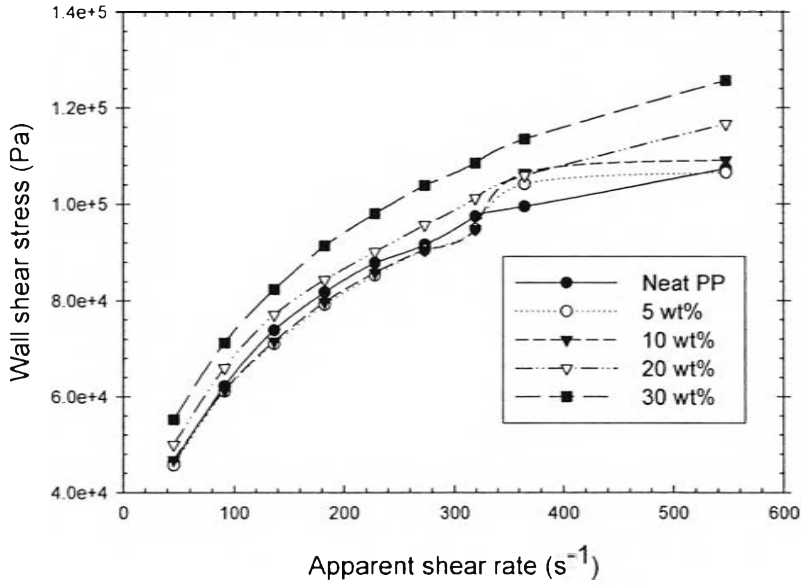
1.4e+5
1.2e+5
1.0e+5
8.0e+4
6.0e+4
4.0e+4
Wall shear stress (Pa)
0
100
200
300
400
500
600
Apparent shear rate (s-1)
Neat PP
5 wt%
10 wt%
20 wt%
30 wt%

(c)

Figure 6.1

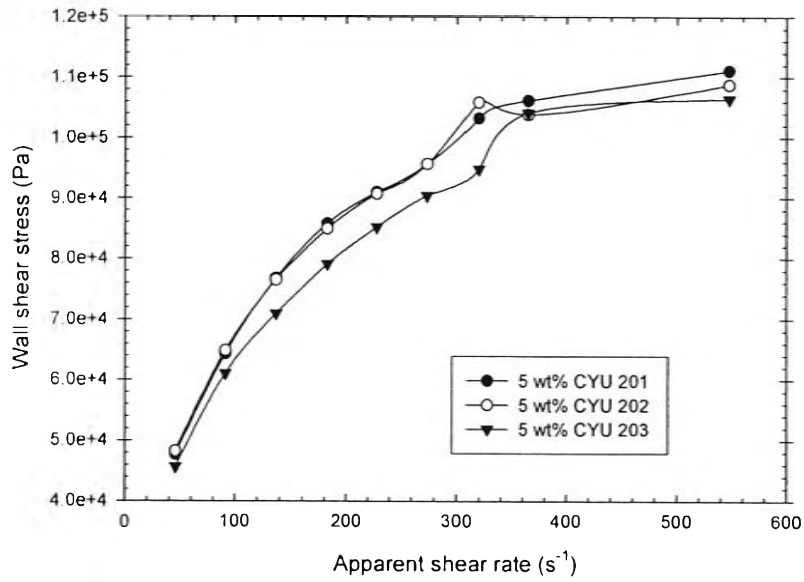
1.2e+5
1.1e+5
1.0e+5
9.0e+4
8.0e+4
7.0e+4
6.0e+4
5.0e+4
4.0e+4
Wall shear stress (Pa)
0
100
200
300
400
500
600
Apparent shear rate (s-1)
5 wt% CYU 201
5 wt% CYU 202
5 wt% CYU 203

(a)

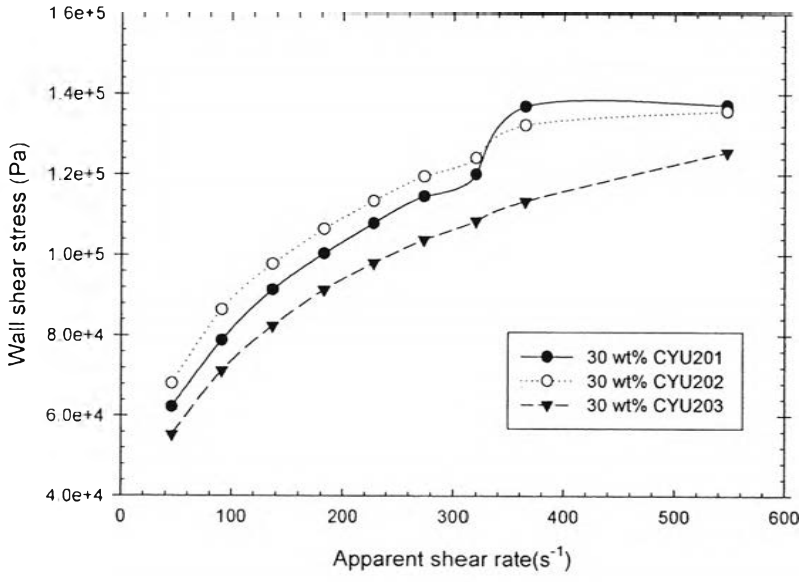
1.6e+5
1.4e+5
1.2e+5
1.0e+5
8.0e+4
6.0e+4
4.0e+4
Wall shear stress (Pa)
0
100
200
300
400
500
600
Apparent shear rate(s-1)
30 wt% CYU201
30 wt% CYU202
30 wt% CYU203

(b)

Figure 6.2

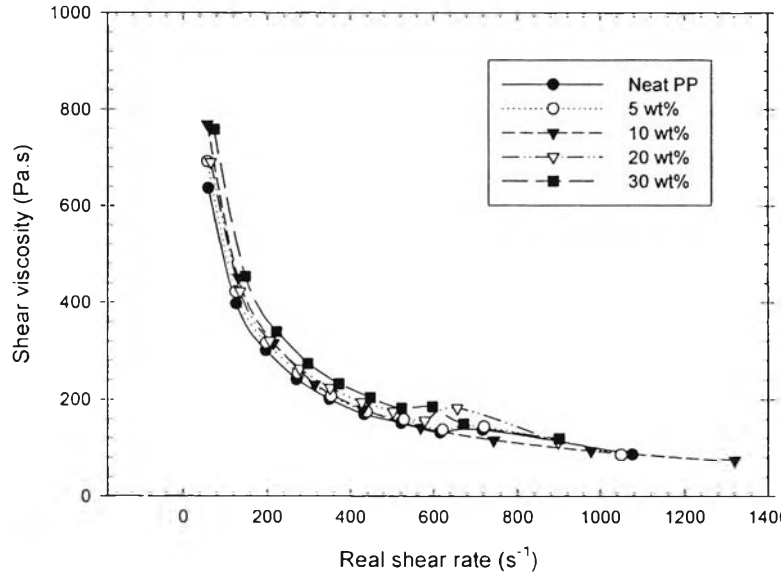
Neat PP
5 wt%
10 wt%
20 wt%
30 wt%
Shear viscosity (Pa.s)
Real shear rate (s-1)
0
200
400
600
800
1000
1200
1400

(a)

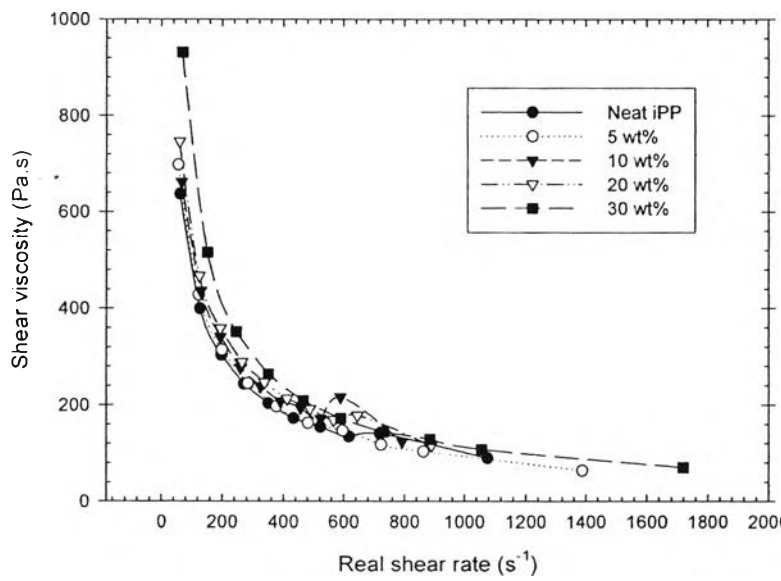
Neat iPP
5 wt%
10 wt%
20 wt%
30 wt%
Shear viscosity (Pa.s)
Real shear rate (s-1)
0
200
400
600
800
1000
1200
1400
1600
1800
2000

(b)

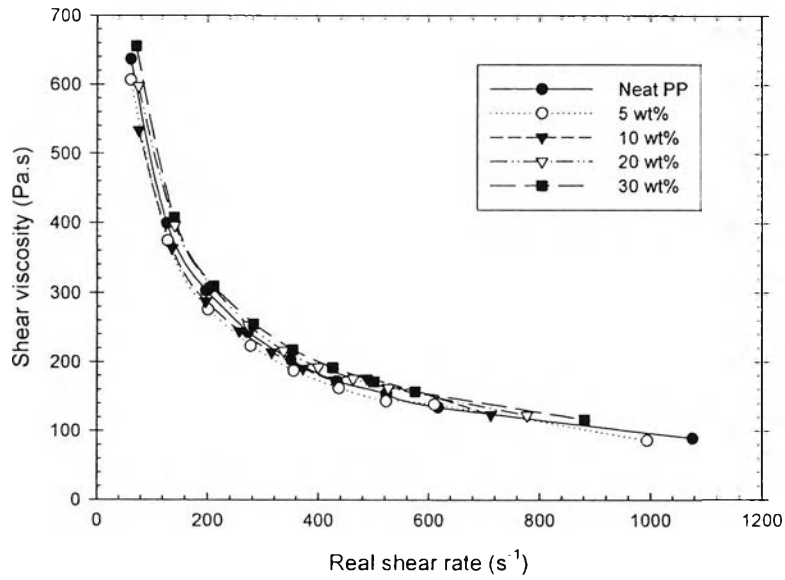
Shear viscosity (Pa.s)
Real shear rate (s-1)
Neat PP
5 wt%
10 wt%
20 wt%
30 wt%
0
100
200
300
400
500
600
700
0
200
400
600
800
1000
1200

(c)

Figure 6.3

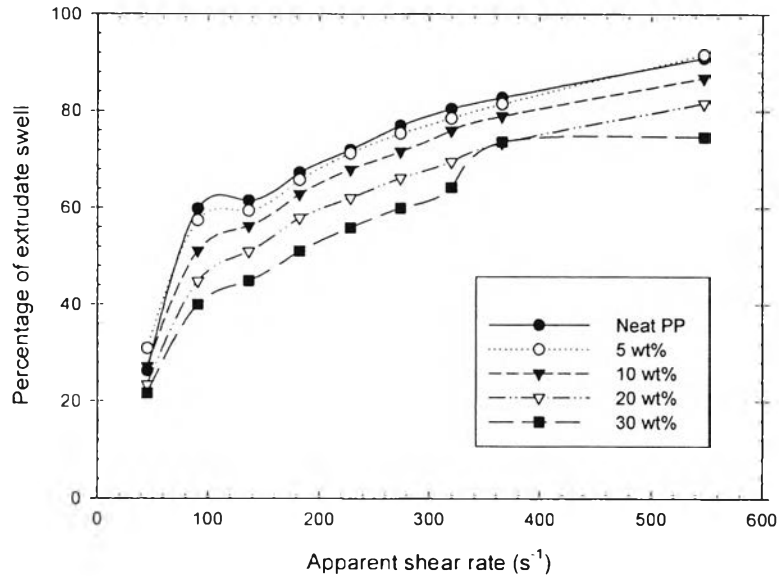
Percentage of extrudate swell
Apparent shear rate (s^{-1})
Neat PP
5 wt%
10 wt%
20 wt%
30 wt%
0
20
40
60
80
100
0
100
200
300
400
500
600

(a)

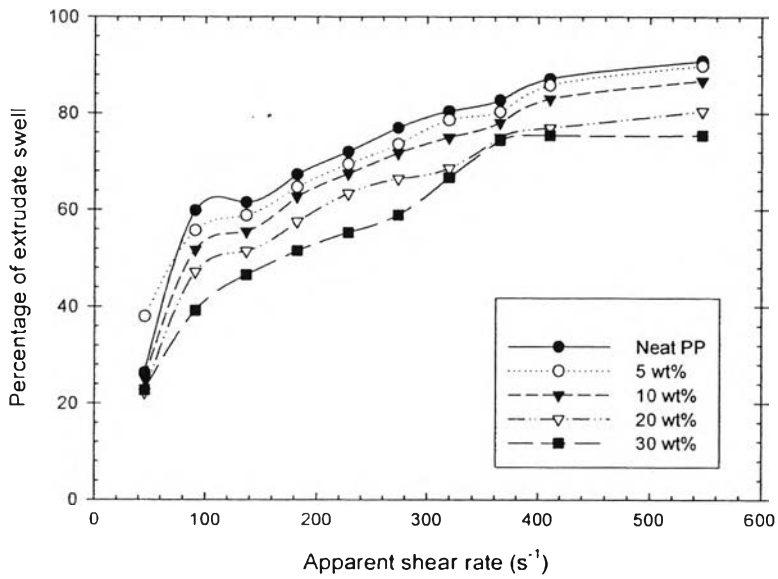
Percentage of extrudate swell
Apparent shear rate (s^{-1})
Neat PP
5 wt%
10 wt%
20 wt%
30 wt%
0
20
40
60
80
100
0
100
200
300
400
500
600

(b)

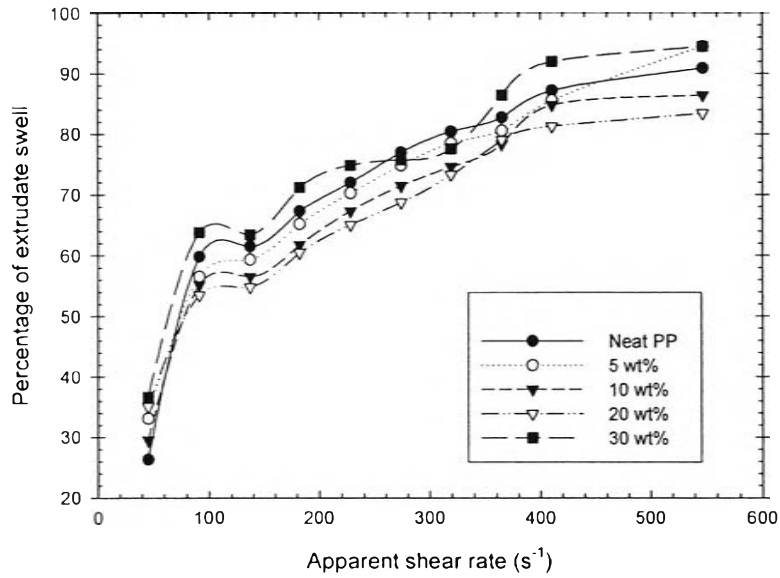
Percentage of extrudate swell
Apparent shear rate (s^{-1})
Neat PP
5 wt%
10 wt%
20 wt%
30 wt%
100
90
80
70
60
50
40
30
20
0
100
200
300
400
500
600

(c)

Figure 6.4

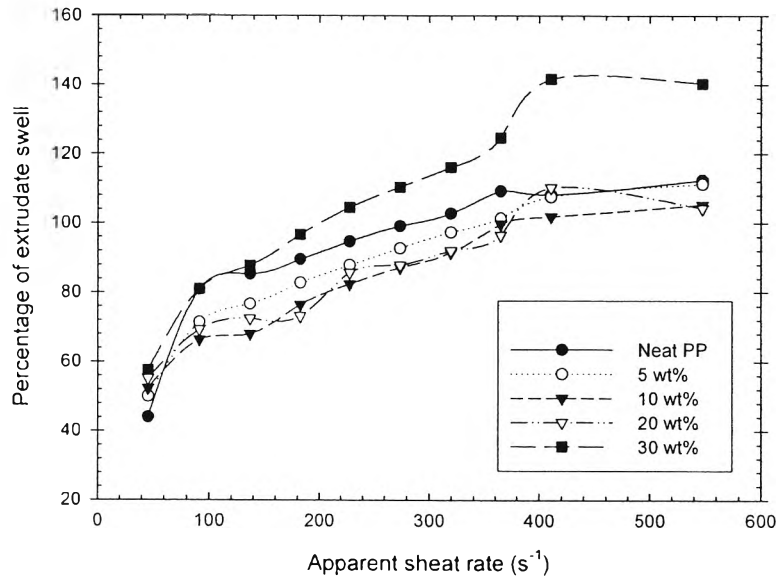
Percentage of extrudate swell
Apparent sheat rate (s^{-1})
160
140
120
100
80
60
40
20
0
100
200
300
400
500
600
Neat PP
5 wt%
10 wt%
20 wt%
30 wt%

Figure 6.5

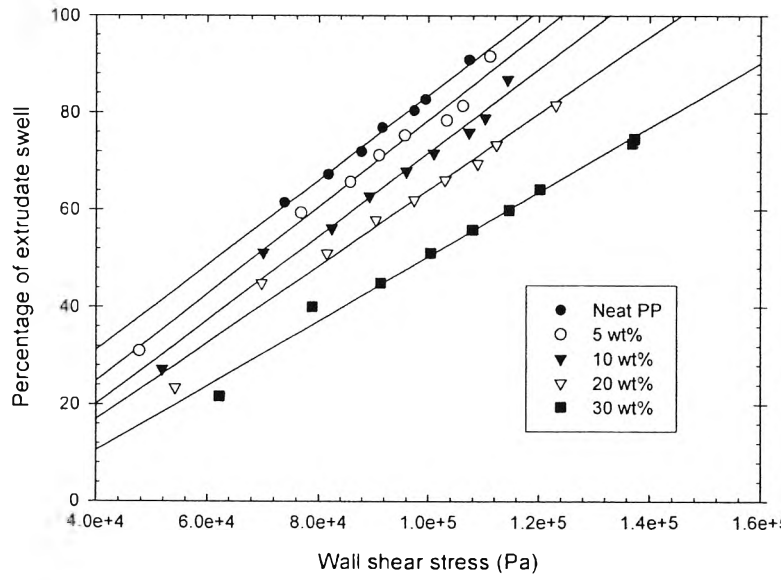
Percentage of extrudate swell
Wall shear stress (Pa)
Neat PP
5 wt%
10 wt%
20 wt%
30 wt%
0
20
40
60
80
100
4.0e+4
6.0e+4
8.0e+4
1.0e+5
1.2e+5
1.4e+5
1.6e+5

(a)

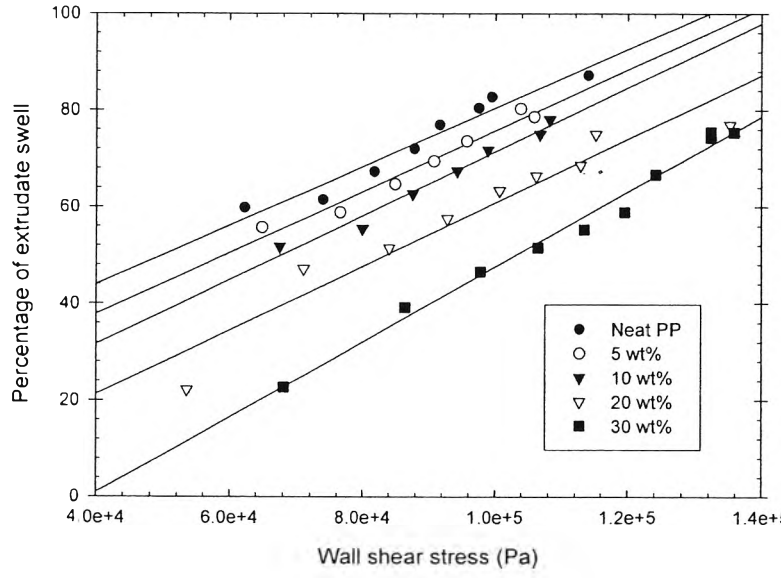
Percentage of extrudate swell
Wall shear stress (Pa)
Neat PP
5 wt%
10 wt%
20 wt%
30 wt%
0
20
40
60
80
100
4.0e+4
6.0e+4
8.0e+4
1.0e+5
1.2e+5
1.4e+5

(b)

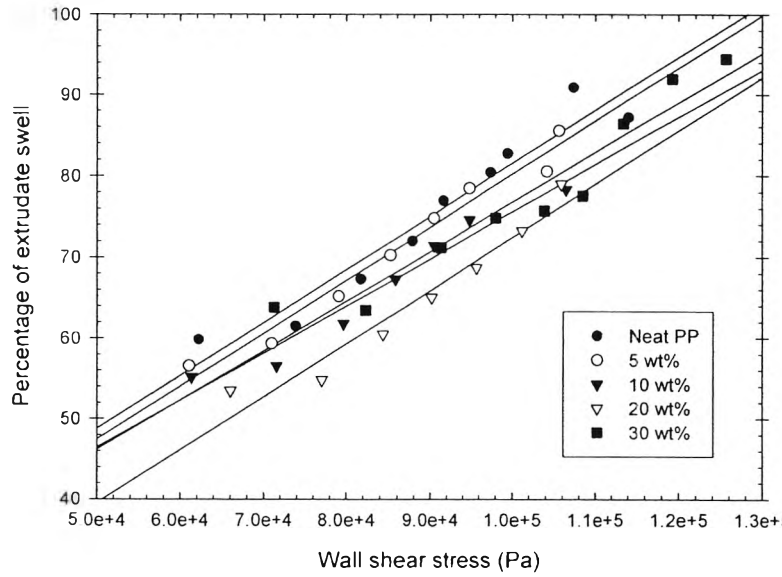
Percentage of extrudate swell
100
90
80
70
60
50
40
5.0e+4
6.0e+4
7.0e+4
8.0e+4
9.0e+4
1.0e+5
1.1e+5
1.2e+5
1.3e+5
Wall shear stress (Pa)
Neat PP
5 wt%
10 wt%
20 wt%
30 wt%

(C)

Figure 6.6

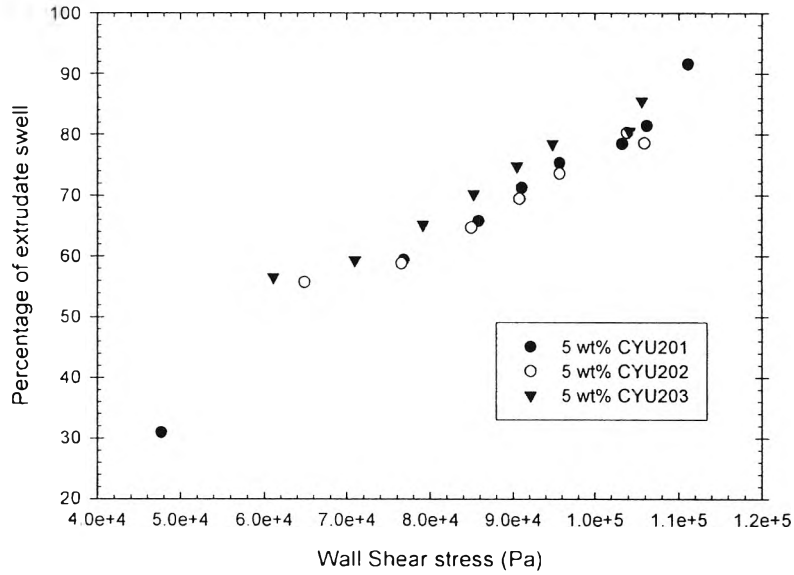
Percentage of extrudate swell
Wall Shear stress (Pa)
5 wt% CYU201
5 wt% CYU202
5 wt% CYU203
100
90
80
70
60
50
40
30
20
4.0e+4
5.0e+4
6.0e+4
7.0e+4
8.0e+4
9.0e+4
1.0e+5
1.1e+5
1.2e+5

(a)

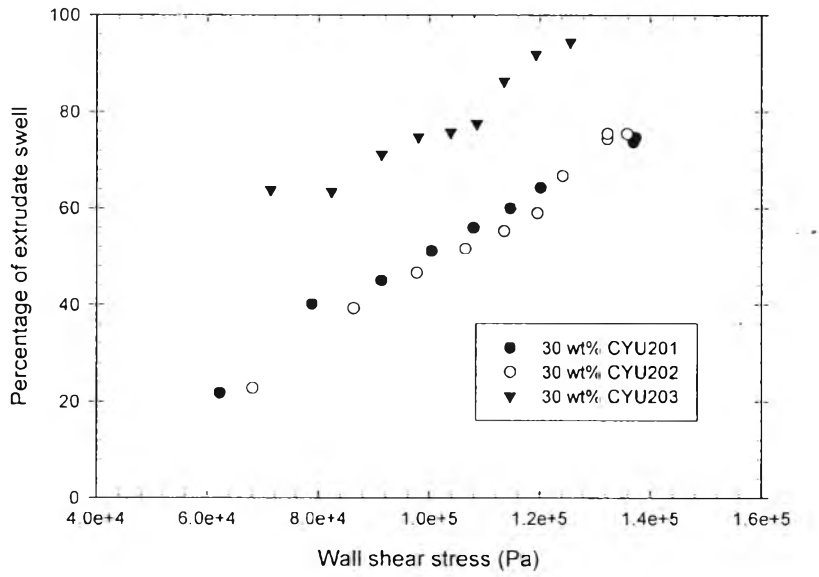
Percentage of extrudate swell
Wall shear stress (Pa)
30 wt% CYU201
30 wt% CYU202
30 wt% CYU203
100
80
60
40
20
0
4.0e+4
6.0e+4
8.0e+4
1.0e+5
1.2e+5
1.4e+5
1.6e+5

(b)

Figure 6.7

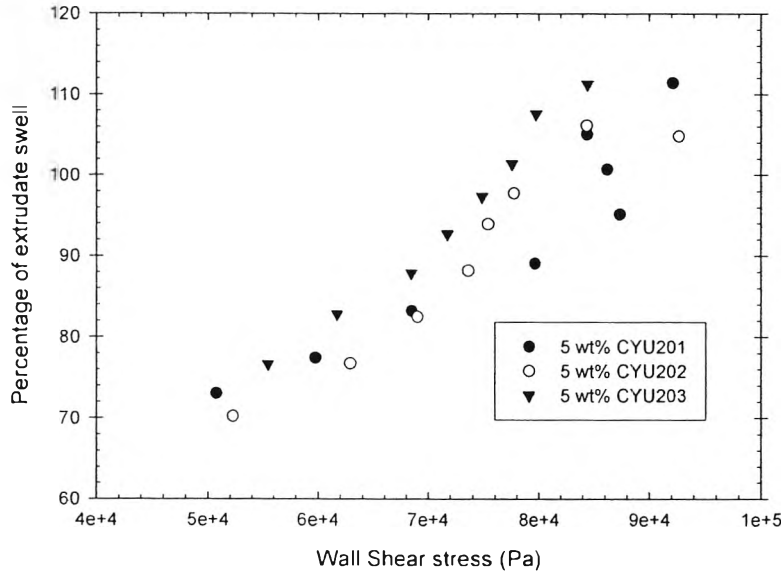
Percentage of extrudate swell
Wall Shear stress (Pa)
5 wt% CYU201
5 wt% CYU202
5 wt% CYU203
120
110
100
90
80
70
60
4e+4
5e+4
6e+4
7e+4
8e+4
9e+4
1e+5

(a)

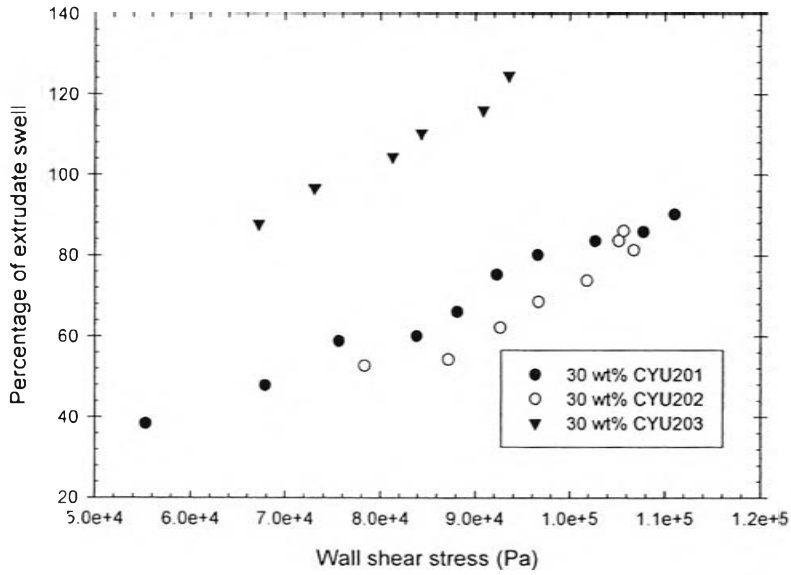
Percentage of extrudate swell
Wall shear stress (Pa)
30 wt% CYU201
30 wt% CYU202
30 wt% CYU203
140
120
100
80
60
40
20
5.0e+4
6.0e+4
7.0e+4
8.0e+4
9.0e+4
1.0e+5
1.1e+5
1.2e+5

(b)

Figure 6.8

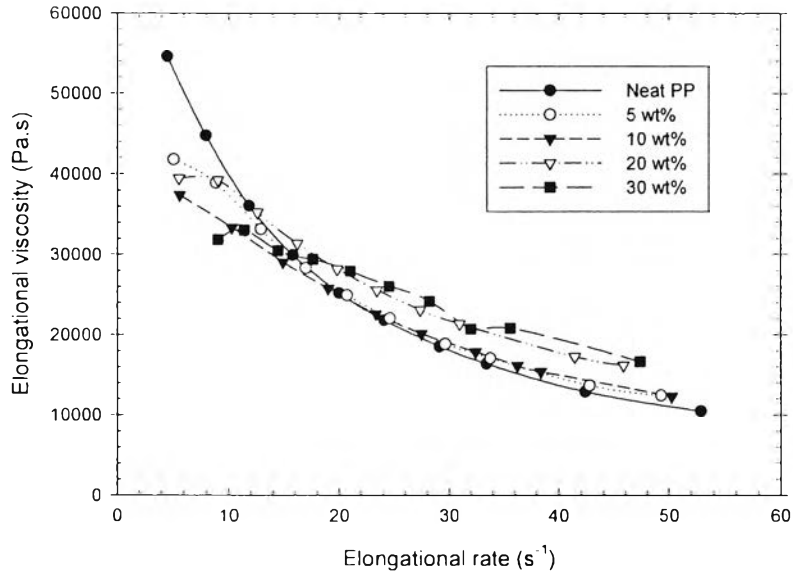
Elongational viscosity (Pa.s)
Elongational rate (s-1)
Neat PP
5 wt%
10 wt%
20 wt%
30 wt%
0
10000
20000
30000
40000
50000
60000
0
10
20
30
40
50
60

Figure 6.9

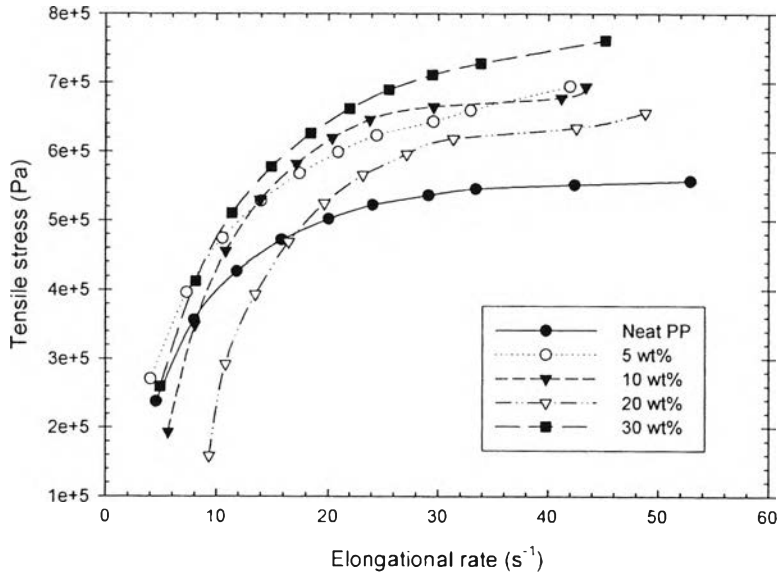
8e+5
7e+5
6e+5
5e+5
4e+5
3e+5
2e+5
1e+5
Tensile stress (Pa)
0
10
20
30
40
50
60
Elongational rate (s-1)
Neat PP
5 wt%
10 wt%
20 wt%
30 wt%

Figure 6.10

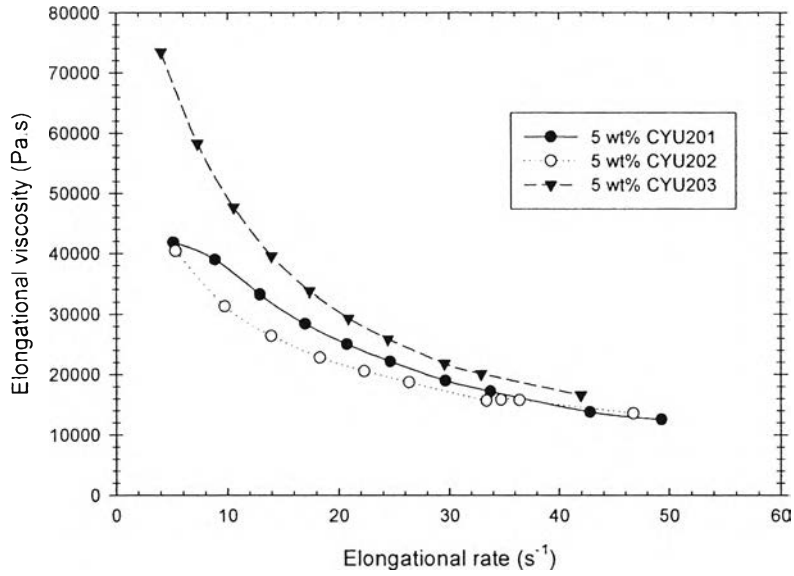

(a)

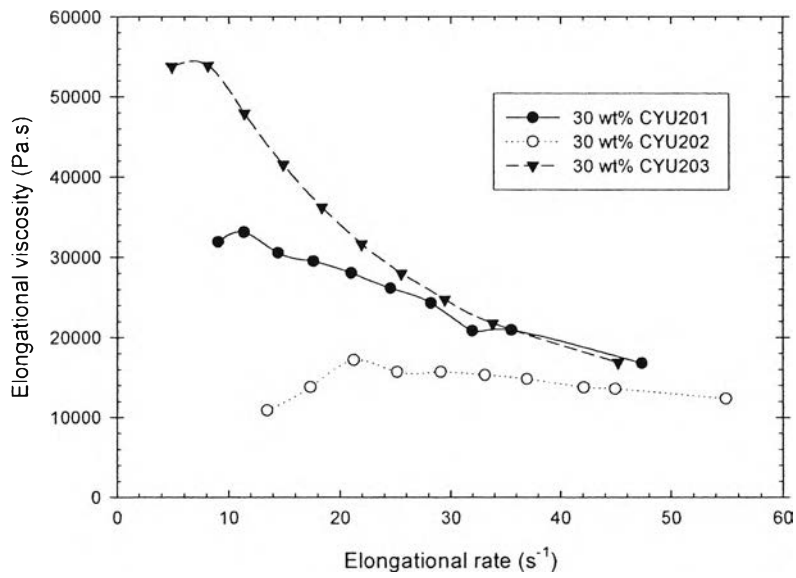

(b)

Figure 6.11

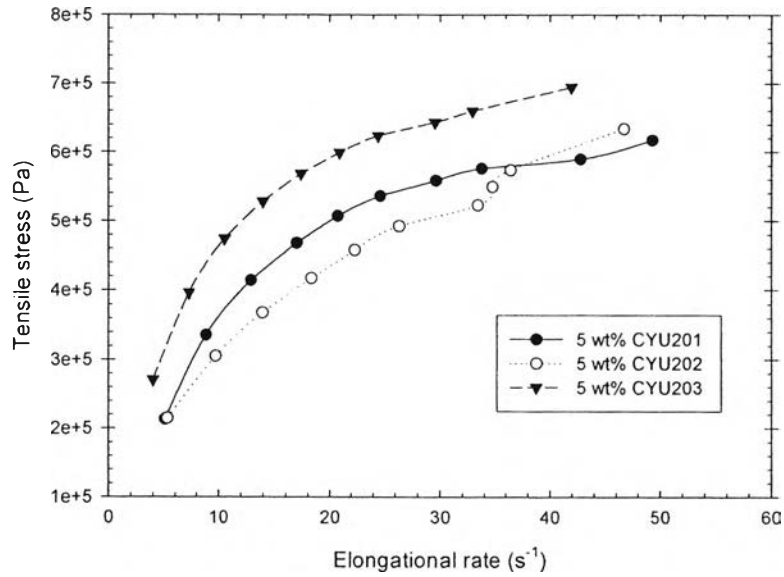

(a)

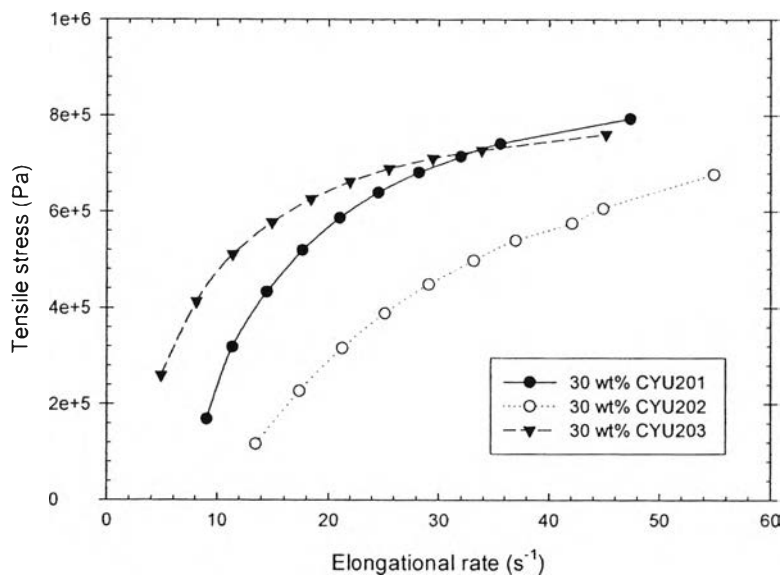

(b)

Figure 6.12